IBRO Reports 8 (2020) 28–35

Contents lists available at ScienceDirect

IBRO Reports

journal homepage: www.elsevier.com/locate/ibror

Research Paper

"Effect of valerenic acid on neuroinflammation in a MPTP-induced mouse model of Parkinson's disease"

Alfredo Rodríguez-Cruz[a,b], Antonio Romo-Mancillas[b,c], Jesus Mendiola-Precoma[a,b], Jesica Esther Escobar-Cabrera[a,b], Guadalupe García-Alcocer[a,b], Laura Cristina Berumen[a,b,*]

[a] Laboratorio de Investigación Genética, Facultad de Química, Universidad Autónoma de Querétaro, Querétaro, Mexico
[b] Posgrado en Ciencias Químico-Biológicas, Facultad de Química, Universidad Autónoma de Querétaro, Querétaro, Mexico
[c] Laboratorio de Diseño Asistido por Computadora y Síntesis de Fármacos, Facultad de Química, Universidad Autónoma de Querétaro, Querétaro, Mexico

ARTICLE INFO

Keywords:
Parkinson´s disease
MPTP
Valerenic acid
C57BL/6J mice
CD-1 mice
Molecular docking
5-HT$_{5A}$

ABSTRACT

Parkinson´s disease is the most important neuromotor pathology due to the prominent loss of dopaminergic neurons in the *substantia nigra pars compacta*. There is an inherent deficiency of dopamine in Parkinson´s disease, which is aggravated when neuroinflammatory processes are present. Several biomolecules are interesting candidates for the regulation of inflammation and possible neuroprotection, such as valerenic acid, one of the main components of *Valeriana officinalis*. A 1-methyl-4-phenyl-1,2,3,6-tetrahydropyridine hydrochloride (MPTP)-induced mouse model of Parkinson's disease was developed to evaluate the motor effects of valerenic acid. The evaluation was carried out with four tests (an invert screen test for muscle strength, cross beam test, open field mobility test and lifting on hind legs test). Subsequently, the neuroinflammatory process was evaluated through ELISA of pro-inflammatory cytokines (IL-1β, IL-6, TNF-α and IFN-γ). The decreases in the inflammatory and neurodegenerative processes were evaluated by Western blot and immunohistochemistry analyses of the tissues, which included an evaluation of the tyrosine hydroxylase and GFAP proteins. Finally, the predicted mechanism of action of valerenic acid was supported by molecular docking calculations with the 5-HT$_{5A}$ receptor. The results indicate that the use of valerenic acid as a co-treatment decreases the neuroinflammation in Parkinson's disease induced by MPTP and provides evidence of a decrease in the evaluated pro-inflammatory cytokines and in the amount of GFAP in the mesencephalic area. Valerenic acid prevents neuroinflammation in a Parkinson's disease mouse model, which might reflect the neuroprotection of dopaminergic neurons with the recovery of motor ability.

Introduction

Parkinson´s disease (PD) is the second-most frequent neurodegenerative disorder after Alzheimer´s disease. PD is the main neuromotor pathology that develops due to the prominent loss of dopaminergic neurons in *substantia nigra pars compacta*, which causes dopamine deficiency (Poewe et al., 2017; Ray Dorsey et al., 2018). The molecular mechanisms of the pathogenesis of PD are diverse, resulting in subtypes of the disease, and they include proteinopathy related to α-synuclein (misfolding and aggregation contributing to Lewy bodies and neurites), oxidative stress, mitochondrial dysfunction and neuroinflammation, which feeds neurotoxic processes (Tansey and Goldberg, 2011; Ganguly et al., 2017; Goswami et al., 2017). Neuroinflammation is an important part of PD development, and microglia play a role in the degradation of α-synuclein and neuronal debris by phagocytosis, which is neuroprotective in balanced activation. The initial activities of pro- and anti-inflammatory factors, which include cytokines, chemokines, and reactive oxygen and nitrogen species, trigger the neuron repair processes, and the early inflammatory process might be beneficial to the neurodegenerative process, including the activation of M2 microglia, which allows suitable control of the elimination of cell debris and α-synuclein protein aggregates. However, the constant presence of α-synuclein protein aggregates leads to a prolonged and unregulated activation of the inflammatory process, with a large amount of cytokines and reactive oxygen species that will trigger more neuronal apoptosis, contributing negatively to the neurodegenerative process of the disease

Abbreviations: PD, Parkinson´s disease; TH, tyrosine hydroxylase; V.A., valerenic acid; MPTP, 1-methyl-4-phenyl-12,3,6-tetrahidropyridine; PBS, phosphate buffered solution; GFAP, glial fibrillary acid protein; LSD, lysergic acid diethylamide

* Corresponding author at: Laboratorio de Investigación Genética, Facultad de Química, Universidad Autónoma de Querétaro, Querétaro, Mexico.
E-mail address: lcbsq@yahoo.com (L.C. Berumen).

https://doi.org/10.1016/j.ibror.2019.12.002
Received 7 May 2019; Accepted 11 December 2019

(Phani et al., 2012; Moehle and West, 2015; Wang et al., 2015; Goswami et al., 2017).

The *Valeriana officinalis* rhizomes used in traditional medicine for anxiety, sleep disorders and anticonvulsant treatment also have reported anti-inflammatory effects. One of the main components of *V. officinalis* essential oil is valerenic acid and it might be responsible for some of the biological properties of *V. officinalis* (Villar del Fresno and Accame, 2001; Hadley and Petry, 2003). A neuroprotective effect has been shown for valerenic acid in pathologies such as Alzheimer's disease (Malva et al., 2004) and cerebral ischaemia (Yoo et al., 2015). A cytoprotective *in vitro* effect was observed using SH-SY5Y neuroblastoma cells as a rotenone-induced PD model (De Oliveria et al., 2009). In another model of rotenone-induced PD in *Drosophila melanogaster,* treatment with valerenic acid decreased the effect of rotenone on PD induction, restoring superoxide dismutase and catalase mRNA levels, increasing the expression of the tyrosine hydroxylase (TH) gene, and increasing the ability to fly (Sudati et al., 2013). Moreover, an anti-inflammatory effect has been attributed to valerenic acid due to its ability to inhibit the NF-κB pathway, which is a promising mechanism for the control of the neuroinflammatory process. Valerenic acid decreased the effect on the NF-κB pathway and the neurodegenerative process through Nrf2 (Jacobo-Herrera et al., 2006; Yamazaki et al., 2015) and modulation of immune cell proliferation (Rodríguez-Cruz et al., 2015). According to these data, the aim of this work was to evaluate the effect of valerenic acid on the neuroinflammatory process in a MPTP-induced mouse model of Parkinson's disease.

Materials and methods

Chemicals

The neurotoxin 1-methyl-4-phenyl-1,2,3,6-tetrahydropyridine hydrochloride (MPTP) and valerenic acid (V.A.) were purchased from Sigma Aldrich, St Louis, USA. IL-1β, IL-6, TNF-α and IFN-γ mini ABTS ELISA development kits (Cat#: 900-M47, 900-M50, 900-M54 and 900-M98, respectively) were purchased from PeproTech®, Rocky Hill, NJ, USA.

Animals and drug treatment

Thirty-two male C57BL/6 J mice and forty male CD-1 mice (body weight 25–30 g and 8 to 10 months old) were purchased from the Institute of Neurobiology, UNAM at Juriquilla, Querétaro, México. The animals were housed at the Animal Department in the School of Chemistry of the Autonomous University of Querétaro (UAQ), México; under a 12 h light/ 12 h dark cycle at 25 °C with water and food given *ad libitum*. The animals used in this study were kept in accordance with the bioethics protocols of UAQ, and the official regulation, NOM-062-ZOO-1999. The study was approved by the Bioethical Committee of the School of Natural Sciences, UAQ (58FCN2016). Four groups per strain of mice were used (minimumapproved for strain) with each group containing eight (n = 8) C57BL/6 J mice or ten (n = 10) CD-1 mice. The control group (1) received saline *i.p*. once a day for seven consecutive days; the MPTP group (2) received MPTP (30 mg/kg body weight, *i.p*) once a day for seven consecutive days and served as the PD model, the V.A. + MPTP group (3) PD model was treated with valerenic acid (2 mg/kg body weight, *i.p*) and subsequently administered MPTP once a day for seven consecutive days, and the V.A. control group (4) was treated with only valerenic acid (2 mg/kg body weight, *i.p*) once a day for seven consecutive days. Motor function was evaluated by multiple paradigms, including the beam walking test, the invert screen test for muscle strength and the open field test.

Motor function tests

Invert screen test for muscle stregth

The invert screen test for muscle strength was a modified version of Kondziela's test (Deacon, 2013). Briefly, an inverted screen was built that consisted of a 40 x 40 cm square of wire mesh composed of 12.5 mm squares of wire with a diameter of 1 mm. The screen was surrounded by 4-cm deep wooden supports, which prevented the mouse from occasionally attempting to climb to the other side. The procedure was as follows. The mouse was placed in the centre of the screen, the timer was initiated and the screen was immediately rotated to an inverted position with the mouse head facing downwards. The screen was kept at a constant 40–50 cm above a cushioned surface. The time before falling was registered as the time of permanence, with a maximum of two minutes, and scored by the following: falling between 1–10 s = 1, falling between 11–25 s = 2, falling between 26–60 s = 3, falling between 61–90 s = 4, and falling after 90 s = 5.

Beam walking test

The beam walking test was performed on 3 consecutive days to habituate the mice, and then the *i.p* injections were given to the animals and the test was performed after treatment. This test evaluated the animals´ motor coordination and balance (Brooks and Dunnett, 2009). The apparatus consisted of a 1-m long, 20-mm thick, 20-cm wide wooden beam with a 15-degree slope that was 75 cm high above the ground. The apparatus was formed by two pedestals: the exit platform was at the first pedestal, and the mouse´s home cage was at the second pedestal. These pedestals were attached by the previously described wooden beam. The animals must reach their home from the lowest part of the apparatus, and the total time that the animals were on the beam line and the occasions of imbalance were recorded.

Open field test

The open field test provides a systematic assessment of environmental exploration and locomotor activity in general. The open field apparatus was a 60 x 60 cm wood cube with walls 30 cm high. The field was divided into grid zones of equal size, 15 x 15 cm, by lines drawn on the ground. The 4 central quadrants had a total size of 30 x 30 cm, which was the basal zone, and the exploratory zone was external to the quadrants. For the procedure, the mice were placed one by one in the apparatus at the centre of the field. External movements or noise during the test were avoided to prevent them from affecting the session. The activity time in the exploration quadrants and each time there was a crossing into the exploratory area was counted for a maximum time of 5 min. At the end, the sum of the exploration time was calculated. In addition, the number of times the mouse stood on its hind legs without support from the walls was counted as the animal´s motive force.

Cytokine quantification by ELISA

After the motor function tests, the mice were sacrificed by intraperitoneal administration of sodium pentobarbital. The brains of four mice from each group were dissected and stored at –80 °C for ELISA. Subsequently, the quantification of the pro-inflammatory cytokines IL-1β, IL-6, TNF-α and IFN-γ was carried out according to the manufacturer instructions.

Immunofluorescence

For immunofluorescence, 24 h after the motor tests, the mice were intraperitoneally anaesthetized with sodium pentobarbital (40 mg/kg) and perfused with 4% paraformaldehyde in phosphate buffered solution (PBS). The brains were removed from the skull and post-fixed in

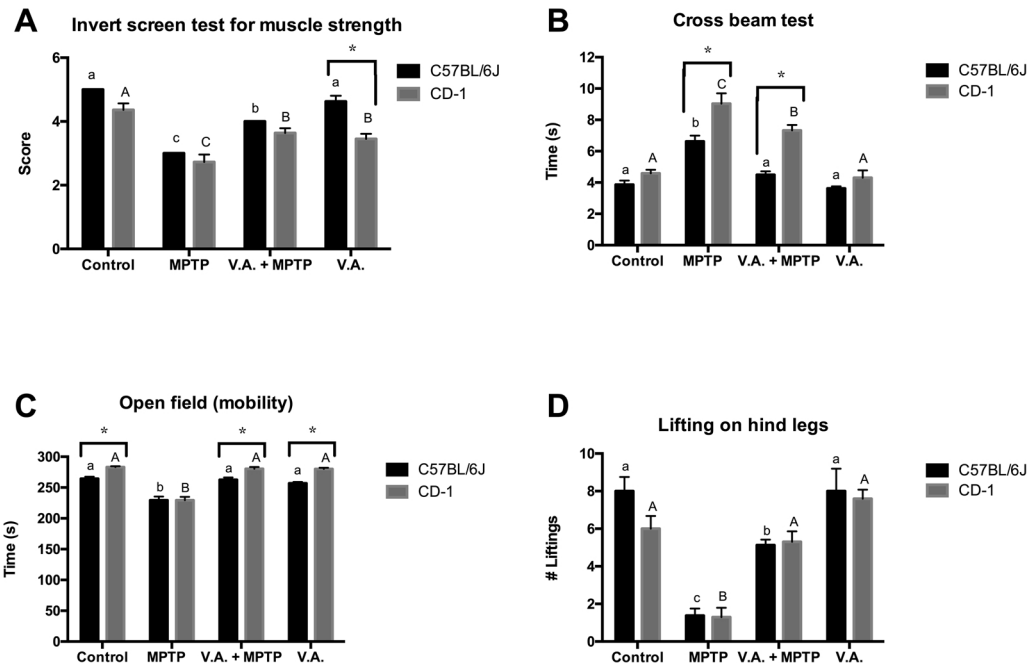

Fig. 1. Motor function test. A. Invert screen test for muscle strength. B. Cross beam test. C. Open field (mobility). D. Lifting on hind legs. The different letters on the bars (mean+/-SEM) represent significant differences between the groups at $p < 0.05$ using two-way ANOVAs with Bonferroni *post-hoc* correction (C57BL/6 J: lowercase letters; CD-1: capital letters) and Sidak-Bonferroni *post-hoc* correction (between strains, *).

4% paraformaldehyde in PBS for 16 h at 4 °C. Subsequently, the brains were washed with PBS and placed overnight in a solution of 30% sucrose in PBS for cryoprotection. Sections were collected from the mesencephalon and mounted in aluminium foil boxes with tissue freezer medium® (Leica, United Kingdom) and frozen at −70 °C until use. The tissue sections were cut on a cryostat (Leica) in 15-µm-thick coronal sections. Sections were incubated with primary antibodies overnight at 4 °C: anti-tyrosine hydroxylase antibody (Millipore AB152, 1:1000) and anti-glial fibrillary acidic protein (GFAP) antibody (Millipore MAB360, 1:500). Alexa Flour® 568-conjugated donkey anti-rabbit IgG (Invitrogen A-10042, 1:1500) and CF™ 488-conjugated goat anti-mouse IgG (Sigma SAB4600238, 1:1500) were the secondary antibodies used with the sections incubated for 2 h at room temperature at 4 °C. Images were acquired on a Zeiss LSM-700 confocal microscope.

Western blot

After obtaining the brains, the midbrain section was dissected and homogenized in a buffer solution (50 mM of Tris−HCl, pH: 9.0–9.5) containing a protease inhibitor cocktail (Roche Diagnostics, Indianapolis, IN). The homogenates were frozen at -70 °C until use. The protein content was determined by the Coomassie Blue test (Bradford). SDS-PAGE was carried out with 150 µg of protein for each sample together with pre-stained molecular weight standards (Bio-Rad, USA) using a 12% gel with a 4% concentrating gel. To complete the electrotransference, the nitrocellulose membranes (Amersham, GE, Germany) were blocked with blotting grade blocker non-fat dry milk (Bio-Rad, USA) in phosphate buffer solution for 2 h. The membranes were then incubated overnight at 4 °C with primary antibodies: anti-tyrosine hydroxylase antibody rabbit (Millipore AB152, 1:1000), anti-glial fibrillary acidic protein (GFAP) antibody mouse (Millipore MAB360, 1:1500), or anti-actin protein antibody goat (Santa Cruz Biotechnology, 1:1000). The membranes were washed and incubated with horseradish peroxidase-conjugated secondary antibodies (anti-mouse 1:750 and anti-rabbit 1:500, Life Technologies; anti-goat 1:500, Invitrogen) for 2 h at room temperature and developed with chemiluminescence prepared for group work. Densitometry analyses were performed using Quantity One Bio-Rad software.

Molecular docking of valerenic acid with the 5HT$_{5A}$ receptor

The molecular docking of valerenic acid with the 5-HT$_{5A}$ receptor was performed to suggest a possible mechanism of action that could explain some of the effects in a MPTP-PD model. Since the three-dimensional structure has not been experimentally resolved, the canonical sequence of the *Mus musculus* 5-HT$_{5A}$ receptor (UniProt P30966) was used to model protein with the GPCR-I-TASSER-webserver (Roy et al., 2010; Yang and Zhang, 2015; Zhang et al., 2017) using the best model predicted by the server for further calculations. The 3D structures of the ligands, such as serotonin, lysergic acid diethylamide (LSD) and valerenic acid, were obtained from Pubchem (CID numbers: 5202, 5761 and 6440940) (National Center for Biotechnology Information, 2019a, 2019b, 2019c). Subsequently, the torsional root and branches of the ligands and the Gasteiger partial charges were assigned using MGLTools 1.5.6 (M.F. Sanner, 1999; Morris et al., 2009), allowing flexibility for all rotatable bonds except the amide bond.

Docking calculations were performed using AutoDock 4.2.6 (Morris et al., 2009) using a search grid box of X:76.185, Y:80.375 and Z:81.624 with a grid spacing of 0.375 Å centred in the transmembrane domain of the receptor. The Lamarckian genetic algorithm was used as a search method for a total of 25 runs with a maximal number of 5,000,000 energy evaluations with 150 conformers as the initial population. The best binding mode for each conformation was analysed using Maestro 2019-1 (Schrödinger, LLC) (Schödinger, 2019).

Data analysis

The statistical analysis was conducted using software Prisma 6. The results are presented as the mean +/- SEM. Two-way ANOVAs with Bonferroni *post-hoc* correction were used to compare all groups of the same strain, and multiple t tests with Sidak-Bonferroni *post-hoc* correction were used to compare both strains of the PD mouse models. Western blot data were analysed with ANOVAs followed by Tukey-Kramer *post-hoc* tests. A *p*-value of less than 0.05 was considered significant.

Results

Motor function tests

According to the motor tests performed (invert screen test for muscle strength, cross beam test, open field mobility and lifting on hind legs), the control groups for the two strains of mice presented an adequate implementation (Nagarajan et al., 2015), and the valerenic acid group did not show any motor effects compared with the control group. This pattern was observed in all motor tests performed (Fig. 1). On the other hand, the PD group (MPTP) had lower scores on the invert screen test for muscle strength, but the MPTP group with valerenic acid treatment (V.A. + MPTP) had increased evaluation time (the evaluated time adjustment score according to Deacon, 2013). The motor behaviours of the different groups are presented for both strains (Fig. 1A). In addition, treatment with valerenic acid, used in the V.A. + MPTP group, produced a significant decrease in the time spent crossing in the walking test on the beam compared to the MPTP group. This pattern was present in both mouse strains (Fig. 1B). Alternatively, in the open field test, the same pattern was shown with improved balance and mobility in the V.A. + MPTP group, compared to the group with Parkinson's disease (MPTP). There was increased mobility time in both strains to behaviour similar to the control group (Fig. 1C). Finally, there was a significant increase in the number of hind leg lifts in the V.A. + MPTP group compared with the PD group, which resulted in an improvement in the motor force with valerenic acid treatment, with similar findings for both mouse strains (Fig. 1D).

Cytokines quantification by ELISA

After analysing the concentration of pro-inflammatory cytokines in the mouse midbrains, an increase in all cytokines (IL-1β, IL-6, TNF-α and IFN-γ) was observed in the MPTP group compared to the control group for both strains. There was a decrease in cytokines in the V.A. + MPTP group while the V.A. group did not change compared to the control group (Fig. 2). The only difference between the strains in the control groups was in IFN-γ (Fig. 2D).

Immunofluorescence and western blot

According to the immunofluorescence and western blot data, the positive tyrosine hydroxylase protein (TH) in the mesencephalon (ventral tegmental area, parabrachial pigmented area) was significantly decreased in the MPTP group (Figs. 3 and 4A). In the V.A. + MPTP group, the data showed an increase in TH labelling, which was confirmed with western blot analyses. The expression of GFAP in the mesencephalon was increased in the MPTP group and decreased in the V.A. + MPTP group according to the immunofluorescence images and the Western blot densitometry analyses (Figs. 3 and 4B), with a similar pattern seen in both mouse strains.

Molecular docking of valerenic acid with the 5HT$_{5A}$ receptor

Molecular docking of valerenic acid with other proteins has been examined, but the suggested interaction with serotonin receptor 5-HT$_{5A}$ has not been reported (Luger et al., 2015; Santos et al., 2016). According to the docking calculations, the main interaction of serotonin with the 5-HT$_{5A}$ receptor occurs at Tyr338 by a π-π interaction with the aromatic ring of serotonin, a hydrogen bond with a hydroxyl group and close contact with residues 70–79 and 338–345; the linear interaction energy obtained was -4.05 Kcal/mol. For LSD, the main interaction occurs by a π-π interaction of the aromatic rings with Phe341 and close contact with residues 70–79 and 338–345; the linear interaction energy obtained was -6.98 Kcal/mol. Finally, valerenic acid had its main interaction with a hydrogen bond between Phe71 and the carboxylic acid of the ligand and close contact with residues 61–65, 71–79 and 338–345; the linear interaction energy obtained was -8.25 Kcal/mol (Fig. 5). These results revealed that the site and the interactions of valerenic acid were similar to those of serotonin and LSD, which are agonists of the 5-HT$_{5A}$ receptor, suggesting that valerenic acid could also be an agonist. These data were consistent with previously reported experimental data (Dietz et al., 2005).

Discussion

The results indicated consistency with the MPTP model of PD reported in the literature by showing a decrease in motor capacity in C57BL/6 J and CD-1 mice. The C57BL/6 J mice were more sensitive to the neurotoxin, resulting in greater motor deficits compared to the CD-1 strain. This observation is to be expected, because, according to Muthane et al. (1994) and Vidyadhara et al. (2017), C57BL/6 J mice, show greater dopaminergic MPTP-neurodegeneration compared to CD-1 mice. Therefore, the results presented in the motor tests (Fig. 1) correlate well with the physiological studies by these authors (Muthane et al., 1994; Vidyadhara et al., 2017). Moreover, the use of the two strains in this study allowed us to observe the responses in the genetic

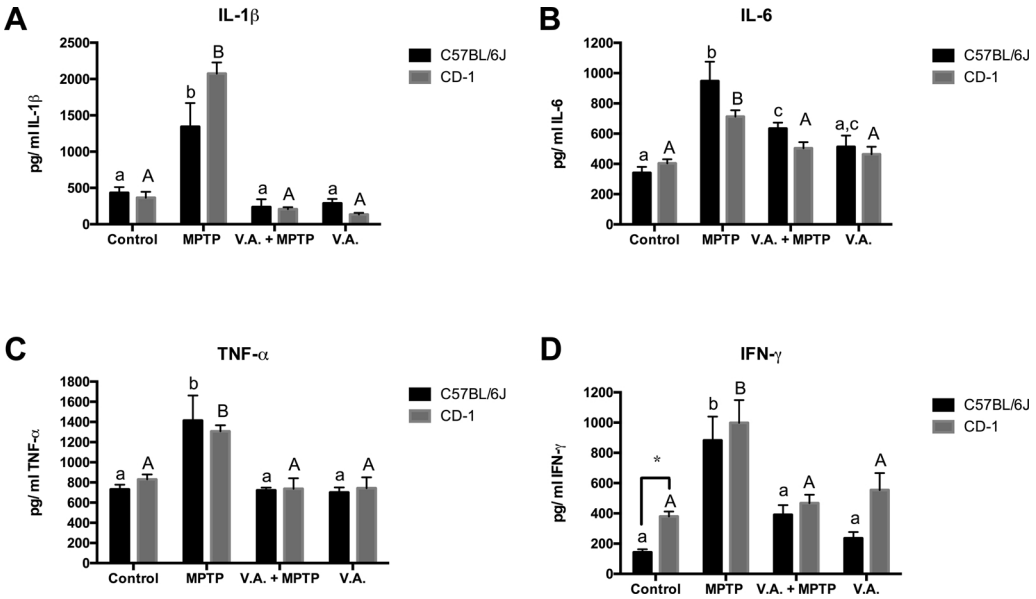

Fig. 2. Cytokine quantification. (A) IL-1-β. (B) IL-6. (C) TNF-α. (D) IFN-γ. The different letters on the bars (mean +/-SEM) represent significant differences between the groups at $p < 0.05$ using two-way ANOVAs with Bonferroni *post-hoc* correction (C57BL/6 J: lowercase letters; CD-1: capital letters) and Sidak-Bonferroni *post-hoc* correction (between strains, *).

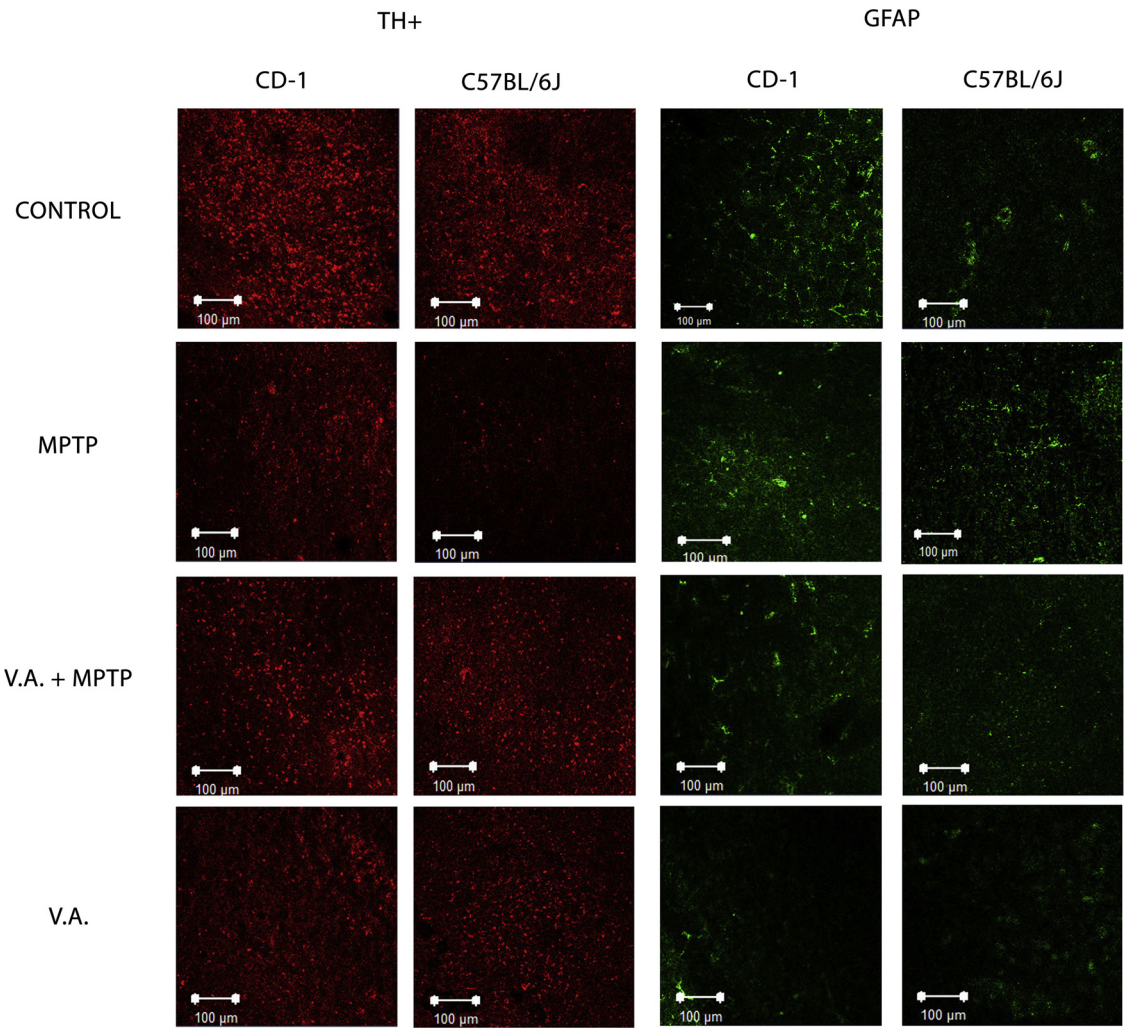

Fig. 3. Expression of Tyrosine Hydroxylase (TH+) and Glial Fibrillary Acidic Protein (GFAP) in the mesencephalon (ventral tegmental area. The figure shows representative images of the two strains (C57BL/6 J and CD-1). MPTP administration to the mice caused the decrease in immunofluorescence of the brain sections, while valerenic acid treatment of MPTP treated mice had similar labelling pattern compared the control group. *Scale bar* 100 µm.

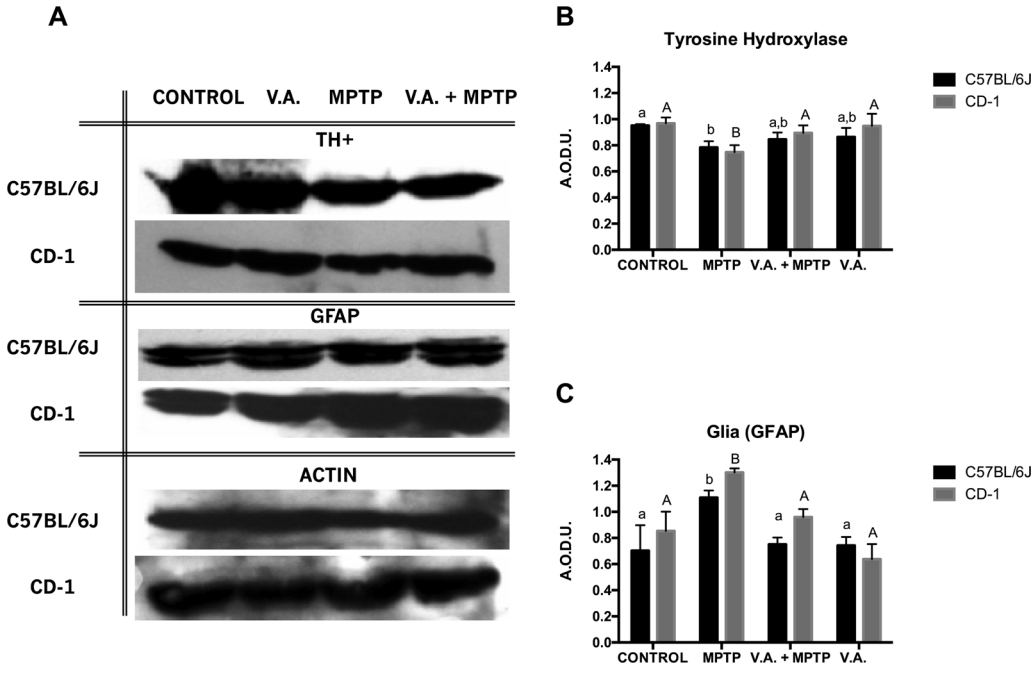

Fig. 4. Western blot quantification of the expression of TH and GFAP proteins in the midbrain. A. Representative immunoblots showing the expression of TH and GFAP proteins in the midbrain. B. Quantitative analysis of TH expression. C. Quantitative analysis of GFAP expression. A.O.D.U: arbitrary optical density units. The different letters on the bars (mean +/-SEM) represent significant differences between the groups at $p < 0.05$ using two-way ANOVAs with Tukey-Kramer *post-hoc* correction (C57BL/6 J: lowercase letters; CD-1: capital letters) and Sidak-Bonferroni *post-hoc* correction (between strains, *).

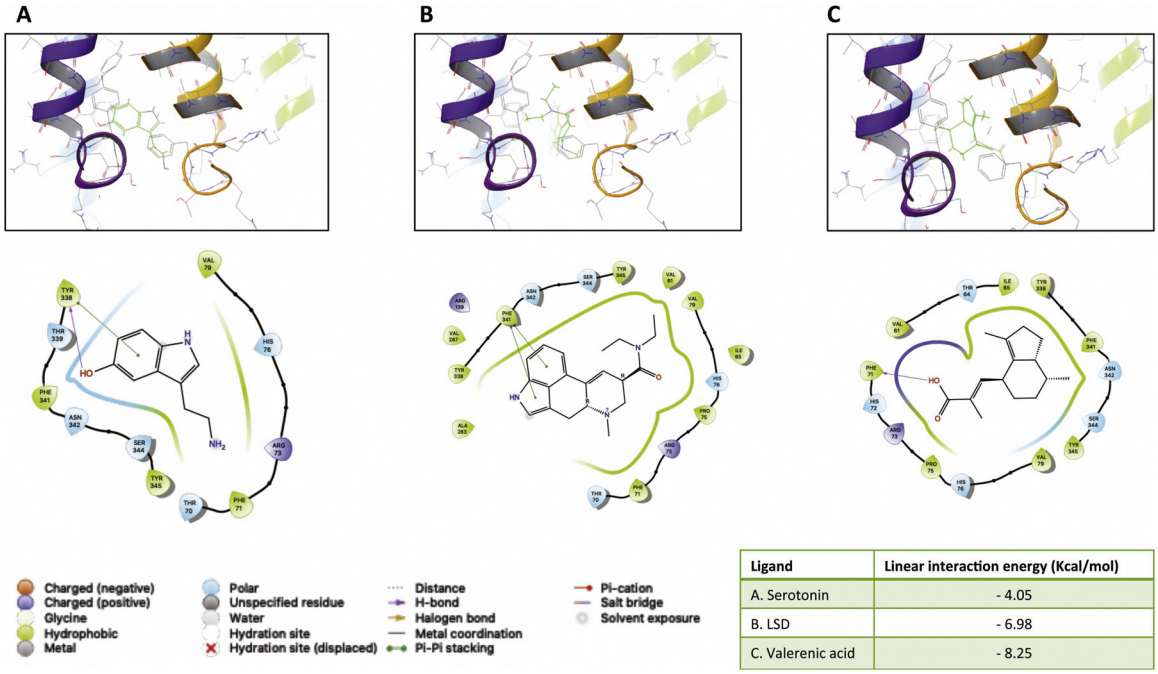

Ligand	Linear interaction energy (Kcal/mol)
A. Serotonin	- 4.05
B. LSD	- 6.98
C. Valerenic acid	- 8.25

Fig. 5. Docking calculation results. Relevant ligand-protein interaction diagrams of the 5-HT_{5A} receptor and the models studied. (A) Serotonin, (B) LSD, (C) Valerenic Acid.

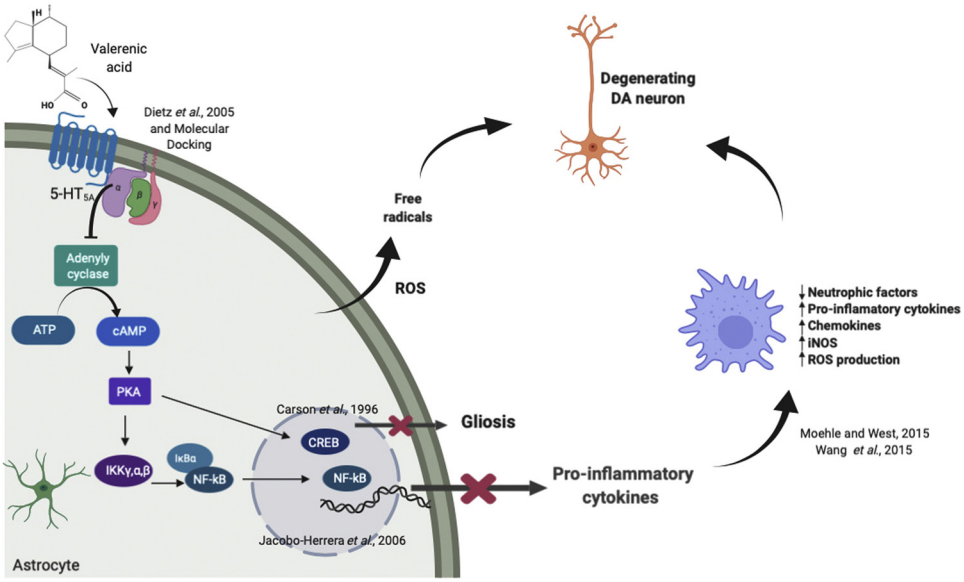

Fig. 6. Proposed mechanism of action of valerenic acid regulating inflammatory processes in a Parkinson´s disease mouse model (created with BioRender.com). Valerenic acid binding to 5-HT_{5A} receptors might activate one of the mechanisms to modulate neuroinflammation processes, inhibiting the cAMP dependent pathway and/or NF-κB pathway, preventing accumulation of pro-inflammatory cytokines and gliosis.

diversity of CD-1 mice (particularly important in pharmacological studies), without detracting from the specific responses for behavioural testing and immunological studies developed with C57BL/6 J mice (Hsieh et al., 2017).

The neuroinflammatory process is a mechanism that plays a very important role in PD. The NF-κB pathway is triggered after microglial cell activation (IFN-γ), with increases in the neurotoxicity of dopaminergic neurons due to the secretion of pro-inflammatory cytokines, such as TNF-α, IL-1β and IL-6 (Arcuri et al., 2017; Sominsky et al., 2018). Increased activity of NF-κB has been observed in dopaminergic neurons in PD (Hunot et al., 1997), and several studies showed that modulation/inhibition of the NF-κB pathway could be a target for controlling PD (Boireau et al., 1997; Ghosh et al., 2007; Flood et al., 2011). In this work, the MPTP group showed an increase in pro-inflammatory cytokines levels (IL-1β, IL-6, TNF-α and IFN-γ) in the midbrain compared to the control group (Fig. 2), which is consistent in aging mice, as observed by Kabel et al., 2018 and Yao and Zhao, 2018. When valerenic acid was used in both mouse strains (C57BL/6 J and CD-1), the concentrations of all evaluated pro-inflammatory cytokines decreased significantly compared to those in the MPTP group. This observation indicates control of inflammation in PD, which is probably related to the inhibition of the NF-κB pathway since valerenic acid has been reported to be an inhibitor of the pathway (Jacobo-Herrera et al., 2006). The decrease in pro-inflammatory cytokines evaluated in both strains of mice was closely related to the decrease in the neuroinflammatory processes, which are considered an important measure of neuroprotection in PD (Gelders et al., 2018).

The neuroprotective effect of valerenic acid was observed by a lower decrease in the amount of tyrosine hydroxylase, a key protein present in dopaminergic neurons. This beneficial effect could be due to

the modulation of neuroinflammatory processes because a decrease in the amount of GFAP, a protein present in the structure of astrocytes, was observed (Figs. 3 and 4) for both strains (C57BL/6 J and CD-1). The studies carried out by the molecular docking calculations showed that valerenic acid could bind to the 5-HT_{5A} receptor as an agonist. This interaction is due to its similarity in binding residues to those of serotonin and LSD calculations (ligands agonists of the 5-HT_{5A} receptor) (Fig. 5). These findings confirm the experimental studies of a valerenic acid agonist association presented by Dietz et al., 2005. The 5-HT_{5A} receptors are highly expressed in astrocytes, inhibiting cAMP accumulation and suppressing the reactivity of astrocytes. This modulation of glial cells and astrocytes can be tracked to the agonistic binding of valerenic acid to the 5-HT_{5A} serotonergic receptors (Carson et al., 1996). In the same way that 5-HT_{1A} serotonergic receptors in astrocytes have been proposed for treatment of Parkinson's disease, the binding of valerenic acid to 5-HT_{5A} receptors could be part of the mechanism (Fig. 6) of the modulation of the neuroinflammatory processes through astrocytes, coupled with the inhibition of NF-κB, which would have a neuroprotective effect (Miyazaki and Asanuma, 2016).

Conclusion

This work presents evidence of valerenic acid´s (the main component of the essential oil from *V. officinalis*) regulation of neuroinflammatory processes in MPTP-induced Parkinson's disease. This reduced neuroinflammation may be achieved through inhibition of NF-κB and activation of the 5-HT_{5A} receptor by its agonist valerenic acid in astrocytes. Valerenic acid is a potent candidate for pretreatment to reduce the incidence and progression of Parkinson's disease.

Conflict of interest

The authors declare no conflicts of interest.

Acknowledgments

The authors would like to thank UAQ for financial support through FOPER-UAQ and the Mexican Council for Science and Technology (CONACYT) for doctoral scholarship number 298061 to A.R-C. The authors also thank the technical assistance from Alicia Irasema Mendieta-Trejo, Elizabeth Martínez-Rojo and Elizabeth Barajas-Conejo.

References

Arcuri, C., Mecca, C., Bianchi, R., Giambanco, I., Donato, R., 2017. The pathophysiological role of microglia in dynamic surveillance, phagocytosis and structural remodeling of the developing CNS. Front. Mol. Neurosci. 10, 1–22. Available at: http://journal.frontiersin.org/article/10.3389/fnmol.2017.00191/full.

Boireau, A., Bordier, F., Dubédat, P., Pény, C., Impérato, A., 1997. Thalidomide reduces MPTP-induced decrease in striatal dopamine levels in mice. Neurosci. Lett. 234, 123–126.

Brooks, S.P., Dunnett, S.B., 2009. Tests to assess motor phenotype in mice: a user's guide. Nat. Rev. Neurosci. 10, 519–529. Available at: http://www.ncbi.nlm.nih.gov/pubmed/19513088.

Carson, M.J., Thomas, E.A., Danielson, P.E., Sutcliffe, J.G., 1996. The 5-HT(5A) serotonin receptor is expressed predominantly by astrocytes in which it inhibits cAMP accumulation: a mechanism for neuronal suppression of reactive astrocytes. Glia 17, 317–326.

Deacon, R.M.J., 2013. Measuring the strength of mice. J. Vis. Exp. 1–4. Available at: http://www.jove.com/video/2610/measuring-the-strength-of-mice.

De Oliveria, D.M., Barreto, G., De Andrade, D.V.G., Saraceno, E., Aon-Bertolino, L., Capani, F., Dos Santos El Bachá, R., Giraldez, L.D., 2009. Cytoprotective effect of valeriana officinalis extract on an in vitro experimental model of parkinson disease. Neurochem. Res. 34, 215–220.

Dietz, B.M., Mahady, G.B., Pauli, G.F., Farnsworth, N.R., 2005. Valerian extract and valerenic acid are partial agonists of the 5-HT 5a receptor in vitro. Brain Res. Mol. Brain Res. 138, 191–197.

Flood, P.M., Qian, L., Peterson, L.J., Zhang, F., Shi, J.S., Gao, H.M., Hong, J.S., 2011. Transcriptional factor NF-κb as a target for therapy in Parkinson's disease. Parkinsons Dis. 2011, 11–14.

Ganguly, G., Chakrabarti, S., Chatterjee, U., Saso, L., 2017. Proteinopathy, oxidative stress and mitochondrial dysfunction: cross talk in alzheimer's disease and parkinson's disease. Drug Des. Devel. Ther. 11, 797–810.

Gelders, G., Baekelandt, V., Van der Perren, A., 2018. Linking Neuroinflammation and neurodegeneration in Parkinson's disease. J. Immunol. Res. 2018, 1–12.

Ghosh, A., Roy, A., Liu, X., Kordower, J.H., Mufson, E.J., Hartley, D.M., Ghosh, S., Mosley, R.L., Gendelman, H.E., Pahan, K., 2007. Selective inhibition of NF-kappaB activation prevents dopaminergic neuronal loss in a mouse model of Parkinson's disease. Proc. Natl. Acad. Sci. U. S. A. 104, 18754–18759. Available at: http://www.ncbi.nlm.nih.gov/pubmed/18000063.

Goswami, P., Joshi, N., Singh, S., 2017. Neurodegenerative signaling factors and mechanisms in Parkinson's pathology. Toxicol. Vitr. 43, 104–112. https://doi.org/10.1016/j.tiv.2017.06.008. Available at:.

Hadley, S., Petry, J.J., 2003. Valerian. Am. Fam. Phys. 67, 1755–1758.

Hsieh, L.S., Wen, J.H., Miyares, L., Lombroso, P.J., Bordey, A., 2017. Outbred CD1 mice are as suitable as inbred C57BL/6J mice in performing social tasks. Neurosci. Lett. 637, 142–147. https://doi.org/10.1016/j.neulet.2016.11.035. Available at:.

Hunot, S., Brugg, B., Ricard, D., Michel, P.P., Muriel, M.P., Ruberg, M., Faucheux, B.A., Agid, Y., Hirsch, E.C., 1997. Nuclear translocation of NF-kappaB is increased in dopaminergic neurons of patients with parkinson disease. PNAS 94, 7531–7536.

Jacobo-Herrera, N.J., Vartianinen, N., Bremmer, P., Gibbons, S., Koistinaho, J., Heinrich, M., 2006. NF-kB Modulators from Valeriana officinalis. Phytother. Res. 20, 917–919.

Kabel, A.M., Omar, M.S., Alhadhrami, A., Alharthi, S.S., Alrobaian, M.M., 2018. Linagliptin potentiates the effect of L-dopa on the behavioural, biochemical and immunohistochemical changes in experimentally-induced Parkinsonism: role of toll-like receptor 4, TGF-β1, NF-κB and glucagon-like peptide 1. Physiol. Behav. 188, 108–118. https://doi.org/10.1016/j.physbeh.2018.01.028. Available at:.

Luger, D., Poli, G., Wieder, M., Stadler, M., Ke, S., Ernst, M., Hohaus, A., Linder, T., Seidel, T., Langer, T., Khom, S., Hering, S., 2015. Identification of the putative binding pocket of valerenic acid on GABAA receptors using docking studies and site-directed mutagenesis. Br. J. Pharmacol. 172 (22), 5403–5413.

Malva, J.O., Santos, S., Macedo, T., 2004. Neuroprotective properties of Valeriana officinalis extracts (Abstract). Neurotox. Res. 6, 131–140. Available at: http://www.ncbi.nlm.nih.gov/pubmed/15325965%5Cnhttp://www.ebscohost.com.

Miyazaki, I., Asanuma, M., 2016. Serotonin 1A receptors on astrocytes as a potential target for the treatment of Parkinson's disease. Curr. Med. Chem. 23, 686–700.

Moehle, M.S., West, A.B., 2015. M1 and M2 immune activation in Parkinson's Disease: Foe and ally? Neuroscience 302, 59–73.

Morris, G.M., Huey, R., Lindstrom, W., Sanner, M.F., Belew, R.K., Goodsell, D.S., Olson, A.J., 2009. AutoDock4 and AutoDockTools4: automated docking with selective receptor flexibility. J. Comput. Chem. 30, 2785–2791.

Muthane, U., Ramsay, K.A., Jiang, H., Jackson-Lewis, V., Donaldson, D., Fernando, S., Ferrerira, M., Prsedborski, S., 1994. Differences in Nigral Neuron Number and sensitivity to 1-Methyl-4-phenyl-1,2,3,6-tetrahydropyridine in C57/bl and CD-1 mice. Exp. Neurol. 195–204.

Nagarajan, S., Chellappan, D.R., Chinnaswamy, P., Thulasingam, S., 2015. Ferulic acid pretreatment mitigates MPTP-induced motor impairment and histopathological alterations in C57Bl/6 mice. Pharm. Biol. 53, 1591–1601.

National Center for Biotechnology Information (2019a) Serotonin, CID = 5202. PubChem Database.

National Center for Biotechnology Information, 2019b. Lysergide, CID = 5761. PubChem Database Available at: https://pubchem.ncbi.nlm.nih.gov/compound/5761 [Accessed February 25, 2019]. .

National Center for Biotechnology Information, 2019c. Valerenic acid, CID = 6440940. PubChem Database Available at: https://pubchem.ncbi.nlm.nih.gov/compound/6440940 [Accessed February 25, 2019]. .

Phani, S., Loike, J.D., Przedborski, S., 2012. Neurodegeneration and inflammation in parkinson's disease. Parkinsonism Relat. Disord. 18, S207–S209. Available at: http://linkinghub.elsevier.com/retrieve/pii/S1353802011700645.

Poewe, W., Seppi, K., Tanner, C.M., Halliday, G.M., Volkmann, J., Schrag, A., Lang, A.E., 2017. Parkinson disease. Nat. Rev. Dis. Primers 3, 1–21.

Ray Dorsey, E., et al., 2018. Global, regional, and national burden of Parkinson's disease, 1990–2016: a systematic analysis for the Global Burden of Disease Study 2016. Lancet Neurol. 17, 939–953.

Rodríguez-Cruz, A., Mendiola-Précoma, J., Escobar-Cabrera, J., Padilla, K., García-Alcocer, G., Berumen, L., 2015. Inhibition of Jurkat and human peripheral blood mononuclear cells proliferation by serotonin and valerenic acid. Front. Immunol. 6, 4–5. Available at: http://www.frontiersin.org/Community/AbstractDetails.aspx?ABS_DOI=10.3389/conf.fimmu.2015.05.00043.

Roy, A., Kucukural, A., Zhang, Y., 2010. I-TASSER: a unified platform for automated protein structure and function prediction. Nat. Protoc. 5, 725–738.

Sanner, M.F., 1999. Python: a programming language for software integration and development. J. Mol. Graph. Model. 17.

Santos, G., Giraldez-Alvarez, L.D., Ávila-Rodriguez, M., Capani, F., Galembeck, E., Neto, A.G., Barreto, G.E., Andrade, B., 2016. SUR1 Receptor interaction with hesperidin and linarin predicts possible mechanisms of action of Valeriana officinalis in parkinson. Front. Aging Neurosci. 8, 97.

Schödinger (2019) Release 2019-1 Maestro.

Sominsky, L., De Luca, S., Spencer, S.J., 2018. Microglia: key players in neurodevelopment and neuronal plasticity. Int. J. Biochem. Cell Biol. 94, 56–60.

Sudati, J.H., Vieira, F.A., Pavin, S.S., Dias, G.R.M., Seeger, R.L., Golombieski, R., Athayde, M.L., Soares, F.A., Rocha, J.B.T., Barbosa, N.V., 2013. Valeriana officinalis attenuates the rotenone-induced toxicity in drosophila melanogaster. NeuroToxicology 37, 118–126.

Tansey, M.G., Goldberg, M.S., 2011. Neuroinflammation in Parkinson's disease: its role in neuronal death and implications for therapeutic intervention. Neurobiol. Dis. 37, 510–518.

Vidyadhara, D.J., Yarreiphang, H., Raju, T.R., Alladi, P.A., 2017. Admixing of MPTP-

Resistant and susceptible mice strains augments nigrostriatal neuronal correlates to resist MPTP-Induced neurodegeneration. Mol. Neurobiol. 54, 6148–6162.
Villar del Fresno, A., Accame, M., 2001. Valeriana officinalis: Fitoquímica, farmacología, y terapéutica. Farmacia Profesional. pp. 98–106.
Wang, Q., Liu, Y., Zhou, J., 2015. Neuroinflammation in Parkinson's disease and its potential as therapeutic target. Transl. Neurodegener. 4 (19) Available at: http://www.translationalneurodegeneration.com/content/4/1/19.
Yamazaki, H., Tanji, K., Wakabayashi, K., Matsuura, S., Itoh, K., 2015. Role of the Keap1/Nrf2 pathway in neurodegenerative diseases. Pathol. Int. 65, 210–219.
Yang, J., Zhang, Y., 2015. I-TASSER server: new development for protein structure and function predictions. Nucleic Acids Res. 43, W174–W181.
Yao, K., Zhao, Y.F., 2018. Aging modulates microglia phenotypes in neuroinflammation of MPTP-PD mice. Exp. Gerontol. 111, 86–93. https://doi.org/10.1016/j.exger.2018.07.010. Available at:.
Yoo, D.Y., Jung, H.Y., Nam, S.M., Kim, J.W., Choi, J.H., Kwak, Y.-G., Yoo, M., Lee, S., Yoon, Y.S., Hwang, I.K., 2015. Valeriana officinalis extracts ameliorate neuronal damage by suppressing lipid peroxidation in the gerbil hippocampus following transient cerebral ischemia. J. Med. Food 18, 642–647.
Zhang, C., Freddolino, P.L., Zhang, Y., 2017. COFACTOR: improved protein function prediction by combining structure, sequence and protein-protein interaction information. Nucleic Acids Res. 45, W291–W299.